Identification of 4^- states in the $^{14}C(p,n)^{14}N$ reaction at 135 MeV

L. A. C. Garcia, B. D. Anderson, D. M. Manley, A. R. Baldwin, R. Pourang,* E. Steinfelds, and J. W. Watson
Department of Physics and Center for Nuclear Research, Kent State University, Kent, Ohio 44242

R. A. Lindgren and B. L. Clausen,†
Institute of Nuclear and Particle Physics and Department of Physics, University of Virginia, Charlottesville, Virginia 22901

A. D. Bacher and C. C. Foster
Indiana University Cyclotron Facility, Bloomington, Indiana 47405
(Received 5 August 1993; revised manuscript received 14 March 1994)

Neutron time-of-flight spectra were measured for the $^{14}C(p,n)^{14}N$ reaction at 135 MeV with the beam-swinger system at the Indiana University Cyclotron Facility. Excitation-energy spectra and differential cross sections for the observed excitations in this reaction were extracted over the momentum transfer range from 0 to 2.5 fm^{-1}. The goal of this work is to identify the 4^- states in ^{14}N and to determine the isovector transition strengths. The identification of the 4^- states is based on comparisons of the theoretical differential cross sections, performed in a DWIA formalism, with the experimental cross sections and with information from the $^{14}C(e,e')$ reaction. Isospin assignments are based primarily on comparisons of the measured (p,n) and (e,e') isovector strengths. Candidate 4^- states are identified at excitation energies of 8.49 MeV ($T=0$), 13.76 MeV and 19.49 MeV ($T=1$), and 26.61 MeV ($T=2$) in the $^{14}C(p,n)^{14}N$ reaction, and the isovector strengths for the transitions leading to these states are extracted. The observed excitation energies and isovector strengths are in good agreement with the analog $T=1$ and $T=2$ 4^- states observed in the (e,e') reaction. The experimental results are compared with results from shell-model calculations.

PACS number(s): 25.40.Kv, 21.10.Hw, 21.60.Cs, 27.20.+n

I. INTRODUCTION

In this paper we present the results of nuclear structure studies with the $^{14}C(p,n)^{14}N$ reaction at 135 MeV. The $^{14}C(p,n)^{14}N$ reaction provides information that is both supplementary and complementary to the information provided by other reactions on the same nucleus, including the (e,e'), (p,p'), (π,π'), and (n,p) reactions.

If the ground state of ^{14}C is described within a p-shell model, then the 4^- states observed via one-step inelastic scattering are obtained from the $1p_{3/2} \rightarrow 1d_{5/2}$ "stretched" transition. This $1\hbar\omega$ transition clearly transfers maximum $\Delta l = 3$ and $\Delta s = 1$ from the initial 0^+ state to the final 4^- state, hence the name stretched. For the transition from the ground state to the 4^- state, only one nuclear transition density is involved, and it is the same for the different probes except for an isospin coefficient. The quantitative information comes from a measure of the isovector strength obtained from the normalization of the theoretical differential cross section, calculated in a distorted-wave impulse approximation (DWIA) formalism, assuming a $1p_{3/2} \rightarrow 1d_{5/2}$ single-particle transition, to the experimental differential cross section. This information is essential to a combined hadronic and electromagnetic analysis.

Inelastic electron scattering is the best understood reaction for nuclear structure. By choosing a strong transition observed in the (e,e') reaction, one can calibrate the effective interaction relevant for the same transition in a hadronic reaction [1,2]. A large number of studies with the (p,n) [3] and (e,e') [4] reactions conclude that both reactions see the same isovector strength (within 20%) for $1\hbar\omega$ stretched transitions, which implies that the DWIA hadronic theoretical description is accurate at this level; thus, the (p,n) reaction can be used as a spectroscopic tool to study nuclear structure.

Many studies involving stretched transitions have been performed with different probes on nuclei and a complete analysis of the results requires looking at both their common and unique aspects. This is important because each probe has its own nuclear spin-isospin selection rules. In a nucleus with $T \neq 0$ and $T_3 = -T$, an isovector transition that proceeds via $\Delta T_3 = +1$ leads to the three possible isospin values $T+1$, T, and $T-1$ in the residual nucleus. For example the $^{14}C(p,n)^{14}N$ reaction will excite $T=0$, $T=1$, and $T=2$ states in ^{14}N. Similarly, an isovector transition that proceeds via $\Delta T_3 = -1$ [e.g., the (n,p) reaction] leads to states with isospin $T+1$ only, while an isovector transition that proceeds via $\Delta T_3 = 0$ [e.g., the (e,e') or the (p,p') reactions] leads to states with isospin T and $T+1$ in the residual nucleus. The

*Present address: Yale University School of Medicine, Department of Therapeutic Radiology, 333 Cedar St., HRT No. 219, New Haven, CT 06510.
†Present address: Geoscience Research Institute, Loma Linda University, Loma Linda, CA 92350 and Physics Department, La Sierra University, Riverside, CA 92515.

(p,n) reaction can excite only isovector ($\Delta T = 1$) transitions, whereas the (p,p') reaction can excite both isovector and isoscalar ($\Delta T = 0$) transitions. Isoscalar strength can make the identification of isovector strength more difficult, particularly if both the isovector and isoscalar strengths are very fragmented.

Studies of $T = 1$ and $T = 2$ 4^- states in ^{14}C with the (e,e') [5] and (π,π') [6] reactions reveal that the isovector strength to the $T = 1$ states is primarily in the transitions to the states at 11.7 and 17.3 MeV, and the strength to the $T = 2$ states is concentrated in a single transition to the state at 24.2 MeV. The strength to the $J^\pi;T{=}4^-;1$ state at 15.2 MeV, seen in the ^{14}C(π,π') [6] reaction, appears to be almost pure isoscalar. Since the strength to the $4^-;1$ states is both isoscalar and isovector, it is possible to combine information from the (e,e') and (π,π') reactions to separate the $\Delta T = 0$ and $\Delta T = 1$ contributions to the total strength observed. From analyses of the (e,e') measurements [5], approximately 45% of the extreme single-particle model (ESPM) isovector strength is observed for both the transitions to the $4^-;1$ and $4^-;2$ states. The (p,n) reaction will excite also $4^-;0$ states, and will provide an independent test of the isospin assignments and strength observed with other probes. Since the 4^- states are expected to be excited only from the $1p_{3/2} \rightarrow 1d_{5/2}$ stretched transition, the observed isovector strengths provide a test of shell-model calculations that include residual interactions and ground-state correlations.

II. EXPERIMENTAL PROCEDURE

The experiment was performed at the Indiana University Cyclotron Facility (IUCF) with the beam-swinger system. The experimental arrangement was similar to that described previously [7,8]. Neutron kinetic energies were measured by the time-of-flight (TOF) technique. A beam of 135 MeV protons was obtained from the cyclotron in narrow beam bursts typically 350 ps long, separated by 2 μs. The long time between beam bursts was obtained by the use of a small storage ring, referred to as the "stripper loop," between the beam source and the main cyclotron. This long time between beam bursts eliminates "overlap" background from previous beam bursts and greatly reduces the cosmic-ray background as well. Neutrons were detected in three detector stations at 0°, 24°, and 45° with respect to the undeflected proton beam. The neutron detectors were rectangular bars of fast plastic scintillator, 10.2 cm thick. Three separate detectors, each with a scintillator bar 1.02 m long by 0.51 m high, were combined for a total frontal area of 1.55 m^2 in the 0° and 24° stations. Two detectors were used in the 45° station, both with a scintillator bar 1.52 m long by 0.76 m high, for a combined frontal area of 2.31 m^2. Each scintillator bar had tapered plexiglass light pipes attached on its two ends, coupled to 12.76 cm diameter phototubes. Timing signals were derived from each end and were combined in a mean-timer circuit [9] to provide the net timing signal from each detector. Overall time resolutions of about 825 ps were obtained, including contributions from the beam burst width (~350 ps) and energy spread (~400 ps), energy loss in the target (~460 ps), neutron transit times across the 10.2 cm thickness of the detectors (~530 ps), and the intrinsic time dispersion of each detector (~300 ps). This overall time resolution provided an energy resolution of about 320 keV in the first two detector stations and about 450 keV in the widest-angle station. The large-volume neutron detectors were described in more detail previously [10]. Protons from the target and cosmic rays were vetoed by anticoincidence detectors on top of and in front of each array.

Time-of-flight spectra were obtained at 12 angles between 0° and 63°. Spectra from each detector were recorded at many pulse-height thresholds from 5 to 40 MeVee (equivalent-electron energy). Calibration of the pulse-height response of each detector was performed with a ^{228}Th gamma source ($E_\gamma = 2.61$ MeV) and a calibrated fast amplifier. The values of the cross sections extracted for different thresholds were found to be the same within statistical uncertainties.

The target composition was 12.7 mg/cm^2 C of which 79% (atomic percent) is ^{14}C and 21% is ^{12}C, 274 μg/cm^2 CHO. Additionally, the target contained (from windows and binder) 2.2 mg/cm^2 CH and ~80 μg/cm^2 Au.

III. DATA ANALYSIS

Absolute differential cross sections were obtained from the measured spectra using the line shape fitting code ALLFIT [11]. This code parametrizes spectra by a sum of peak-shape functions and a background term. In the present work, the peak shape was described by a Gaussian resolution function. The background term included an instrumental contribution, which was taken to be either a constant or linear function of the inverse velocity. At the nucleon decay threshold of the target there is an abrupt change in the slope of the background. This contribution, which entered only above the threshold, was described by a polynomial of order up to 3 (see Fig. 1).

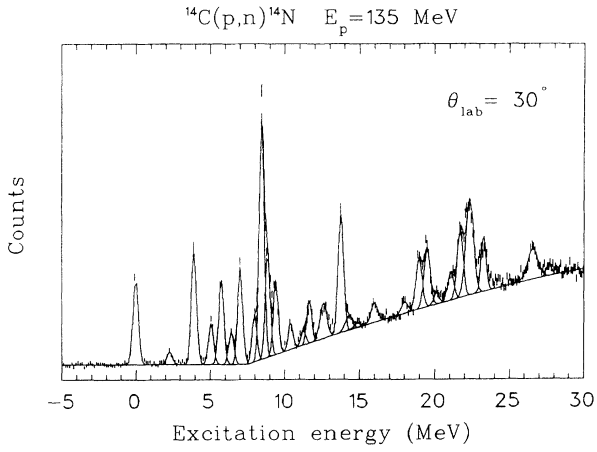

FIG. 1. Fit to a typical (p,n) TOF spectrum, performed with the code ALLFIT. The energy resolution [full width at half maximum (FWHM)] for this spectrum is about 360 keV.

From kinematical considerations and the composition of the ^{14}C target, we were able to identify contaminant peaks from the $^{12}C(p,n)^{12}N$ and $^{16}O(p,n)^{16}F$ reactions (see Fig. 2). Time-of-flight spectra obtained also in this experimental run for the $^{12}C(p,n)^{12}N$ and $^{16}O(p,n)^{16}F$ reactions were fitted, and their contributions to the $^{14}C(p,n)^{14}N$ cross sections subtracted. For each fitted spectrum, two or three peaks of known excitation energy [12] were used to calibrate the inverse velocity scale. Centroids of peaks with known excitation energies were held fixed during the fitting procedure. This method allowed us to determine excitation energies for other peaks to a precision of about ±30 keV. The typical total uncertainty in the extracted cross sections is about 12% and was obtained by combining in quadrature the systematic uncertainties with the statistical uncertainties. In all the cross-section plots, only the statistical uncertainties are shown.

IV. IDENTIFICATION OF THE 4^- STATES

In the approximation that the potential describing the single-particle states is of the harmonic-oscillator form, we can estimate, using a value for the oscillator parameter of $b = A^{1/6} = 14^{1/6} = 1.55$ fm [13], that the differential cross section for a $1p_{3/2} \rightarrow 1d_{5/2}$ stretched transition from the ground state to the 4^- states peaks at about 1.4 fm^{-1}, which corresponds to a laboratory angle of about 30°. Figure 3 shows an excitation-energy spectrum for the $^{14}C(p,n)^{14}N$ reaction at 135 MeV and a laboratory angle of about 30°. The most prominent peaks are located at excitation energies (E_x) of 0.00, 2.31, 3.95, 5.10, 5.78, 7.04, 8.49, 10.43, 11.67, 12.69, 13.76, 15.88, 19.49, 21.5, 22.5, and 26.61 MeV. The peaks observed at 21.5 and 22.5 MeV are known 4^- states in ^{12}N and ^{16}F, respectively. Table I lists the states of ^{14}N we observed at large momentum transfer. Differential cross sections for the states observed were obtained approximately every 6° from 0° to 63°.

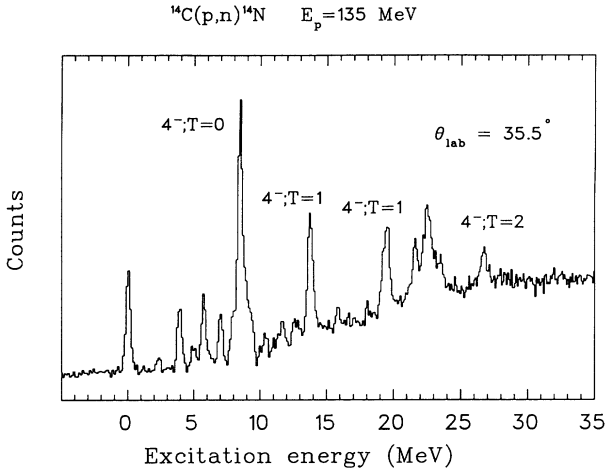

FIG. 3. Excitation-energy spectrum for the $^{14}C(p,n)^{14}N$ reaction at 135 MeV and momentum transfer of about 1.6 fm^{-1}.

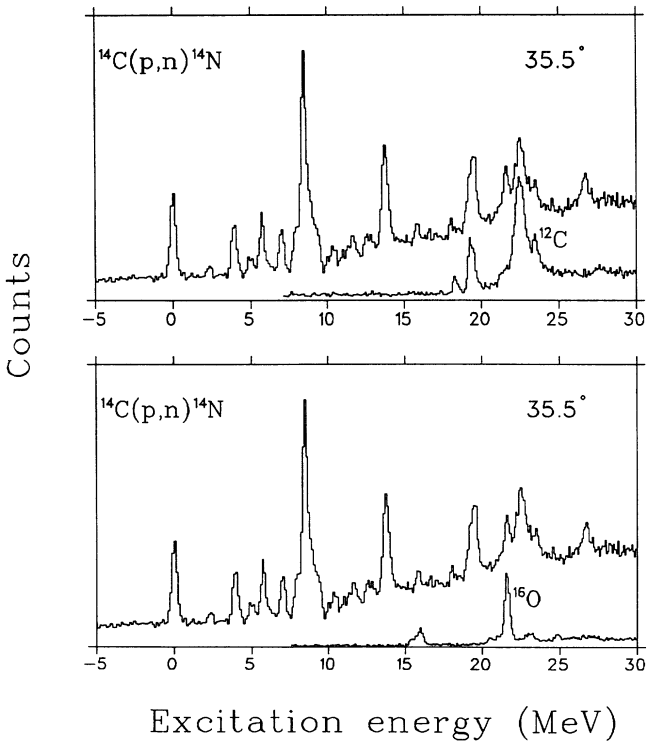

FIG. 2. Excitation-energy spectrum at 35.5° for the $^{14}C(p,n)^{14}N$ reaction at 135 MeV showing the normalized contaminant spectra from the $^{12}C(p,n)^{12}N$ and the $^{16}O(p,n)^{16}F$ reactions.

The theoretical differential cross sections were calculated in the framework of the distorted-wave impulse approximation (DWIA) with the code DW81 [14] assuming a $1p_{3/2} \rightarrow 1d_{5/2}$ single-particle transition. These calculations involve several main ingredients. The microscopic t matrix is from the work of Franey and Love [15] and represents a fit to NN phase shifts at 140 MeV. The optical-model parameters were taken from a $^{12}C(p,p')$ analysis by Comfort and Karp [16], and the parameters of the harmonic-oscillator single-particle states were determined from an (e,e') analysis [5]. Based on previous (p,n) and (e,e') work, we know that the tensor term of the t matrix has the appropriate strength at 135 MeV to describe the projectile-target nucleon coupling. In the plane-wave approximation, the basic shape for the differential cross section of a state excited by the stretched transition of multipolarity J is a polynomial of order $2(J-1)$ in the momentum transfer, q, times a Gaus-

TABLE I. ^{14}N states observed in this work at large momentum transfer.

E_x (MeV)	$J^\pi;T$	E_x (MeV)	$J^\pi;T$
0.00 ± 0.02	$1^+;0$	10.43 ± 0.04	$2^+;1$
2.31 ± 0.02	$0^+;1$	11.67 ± 0.04	$(1^-,2^-)$
3.95 ± 0.02	$1^+;0$	12.69 ± 0.03	$3^-;0$
5.10 ± 0.02	$2^-;0$	13.76 ± 0.04	$1^+,4^-;1$
5.78 ± 0.02	$3^-;0$	15.88 ± 0.03	(4^-)
7.00 ± 0.06	$2^+;0$	19.49 ± 0.05	$4^-;1$
8.49 ± 0.02	$4^-;0$	26.61 ± 0.08	$4^-;2$

sian function of q. We find that the DWIA calculations generally describe the measured differential cross sections well.

In many instances, it happens that the 4^- state cannot be resolved from neighboring states of lower multipolarity. For these cases it is necessary to know the momentum-transfer dependence of the cross section for the lower-multipolarity states. For states with known spin and parity, $0\hbar\omega$ and $1\hbar\omega$ shell-model calculations (Sec. VI) were performed with the code OXBASH [17]. The resultant one-body density-matrix elements (OBDME) were used to calculate the cross sections for these states.

In the following subsections, first we identify the states that are the best 4^- candidates, viz., those at excitation energies of 8.49, 13.76, 19.49, and 26.61 MeV; next we discuss the extraction of the isovector strengths for the $0^+ \rightarrow 4^-$ transitions, and the isopin assignments for the 4^- states.

1. 8.49 MeV T=0 level

At large momentum transfer, the state at 8.49 MeV dominates the spectrum. Near this excitation energy, the ^{14}N spectrum is well known. This state was first assigned to be a 4^- state by Detenbeck *et al.* in the $^{13}C(p,\gamma)^{14}N$ reaction [18]. Figure 4 shows the (p,n) differential cross section for this state. The 4^- DWIA calculation is normalized to the largest experimental value of the cross section, and the shape agrees well with the experimental angular distribution. The code DW81 uses single-particle wave functions of the relative coordinate between the struck nucleon and the $(A-1)$ core. Using single-particle wave functions from the harmonic-oscillator model, the appropriate oscillator parameter b is $b_{\rm rel} = \sqrt{A/(A-1)}b_o$ where b_o is the oscillator parameter for wave functions referred to an arbitrary origin [19]. The oscillator parameter used in this calculation ($b_o = 1.52$ fm) was obtained from an inelastic electron scattering analysis for the $T = 1$ and $T = 2$ 4^- states [5]. No analog of this state was observed in the $^{14}C(e,e')$ reaction [5] at backward angles; hence, as is well known, this state has $T = 0$.

One could argue that since this state is well known, its angular distribution could be used to determine the oscillator parameter independently from the $^{14}C(e,e')$ analysis. In either case the value of $b_{\rm rel}$ would be approximately the same.

2. 13.76 MeV T=1 state

Figure 5 shows the differential cross section for the peak observed at 13.76 MeV and the corresponding DWIA calculation. We believe that this peak is due to an unresolved $(4^-,1^+)$ complex [12]. Their analogs are well resolved in the $^{14}C(e,e')$ experiment, where the $1^+;1$ state is observed at 11.31 MeV and a strong $4^-;1$ state

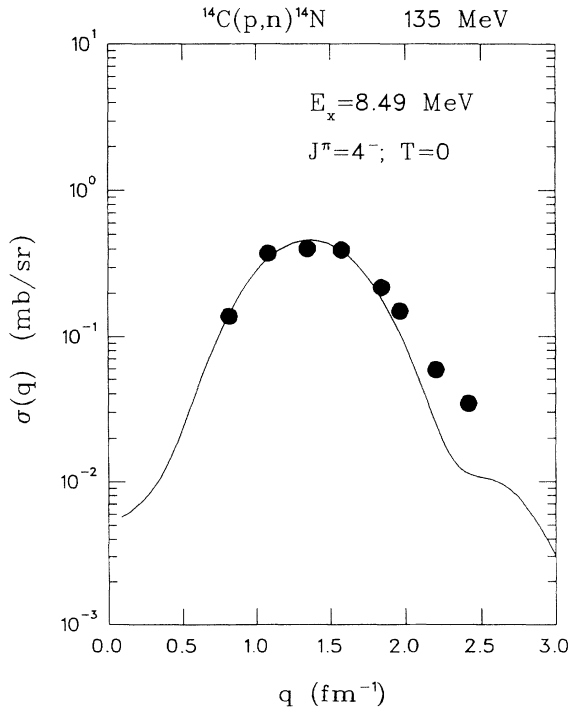

FIG. 4. Differential cross section measured for the 8.49 MeV state in ^{14}N. The curve shows the DWIA calculation for the $1p_{3/2} \rightarrow 1d_{5/2}$ stretched transition from the ground state to the 4^- state, with $b = 1.58$ fm. The isovector transition strength to this state is $Z_1^2(\text{expt}) = 0.22$.

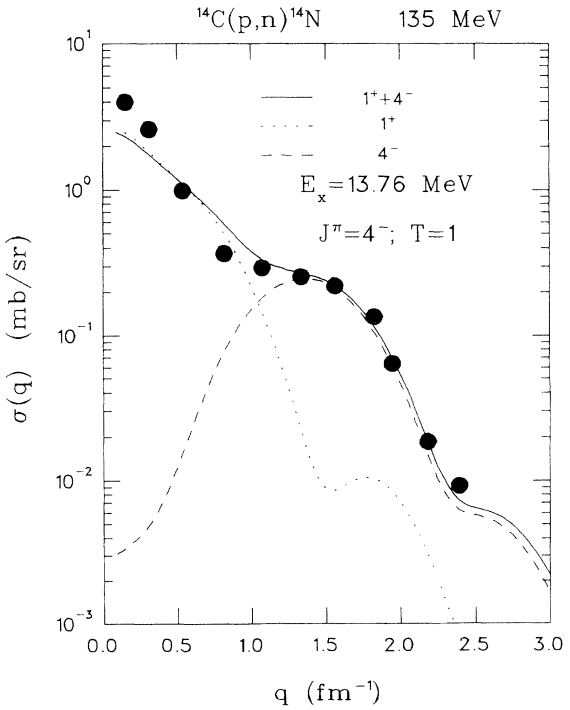

FIG. 5. Differential cross section measured for the 13.76 MeV state in ^{14}N. The curve shows the DWIA calculation for the $1p_{3/2} \rightarrow 1d_{5/2}$ stretched transition from the ground state to the 4^- state, with $b = 1.58$ fm. The isovector transition strength to this state is $Z_1^2(\text{expt}) = 0.10$.

is observed at 11.7 MeV [5]. The 11.7 MeV 4^- state was also observed in a $^{14}C(\pi,\pi')$ experiment [6].

At the $0\hbar\omega$ level, the 1^+ state has a unique $(p_{3/2}^{-1})(p_{1/2}^{-1})$ configuration; thus, it is not surprising that the only strong amplitude from the $2\hbar\omega$ shell-model calculation described in the $^{14}C(e,e')$ paper [5] is the $1p_{3/2} \rightarrow 1p_{1/2}$ amplitude. Since the theoretical form factor with a normalization of 0.39 describes the shape of the low-q (e,e') data well, we may infer that the isovector amplitude for the $1p_{3/2} \rightarrow 1p_{1/2}$ transition is approximately 0.265 22. Using this amplitude in the DWIA calculation for a 1^+ state and adjusting the normalization for the 4^- state produces the cross sections shown in Fig. 5. The agreement for the 13.76 MeV complex is quite good. As a simple check for the amplitude deduced from the (e,e') analysis, we performed a shell-model calculation in a $0\hbar\omega$ space. A single $1^+;1$ level at 11.56 MeV was predicted with a theoretical isovector amplitude of $0.443\,68(p_{1/2},p_{3/2}^{-1})$. To agree well with the experimental (p,n) cross section at low q, a normalization of 0.45 is required; thus, the empirical amplitude is $\sqrt{0.45} \times 0.443\,68 = 0.297\,63$, in good agreement with that deduced from the (e,e') analysis.

3. 19.49 MeV T=1 state

The state at 19.49 MeV is described well by a DWIA calculation (see Fig. 6) assuming a 4^- assignment. Further evidence for the 4^- assignment comes from the $^{14}C(e,e')$ [5] and $^{14}C(\pi,\pi')$ [6] experiments, where the analog of the 19.49 MeV state was observed at 17.3 MeV in ^{14}C. Although there might be a weak unresolved state, the larger cross section observed for the lower-momentum transfer data is likely to be due to some unsubtracted cross section from the contaminant state at 1.12 MeV in ^{12}N (see Fig. 2).

4. 26.61 MeV T=2 state

Figure 7 shows the cross section and the DWIA calculation for the state at 26.61 MeV. We expect the analog of the known $4^-;2$ state in ^{14}B at 2.08 MeV to be at about 26.3 MeV in ^{14}N, which is in good agreement with the state we see at 26.61 MeV. In the $^{14}C(e,e')$ analysis [5], a complex of states appears at 24.4 MeV, and is described as a 4^- and 2^- doublet. A shell-model calculation (see Sec. VI) predicts a 2^- state at 26.2 MeV and we used the OBDME's from this calculation in the DWIA (the single-particle phase conventions used in DW81 and OXBASH are equivalent except that in DW81 the radial wave function is positive at infinity while in OXBASH the radial wave function is positive near the origin). The isovector amplitudes to the $2^-;2$ state are $-0.013\,17(d_{3/2},p_{1/2}^{-1})$, $-0.046\,58(d_{3/2},p_{3/2}^{-1})$, $-0.052\,64(d_{5/2},p_{1/2}^{-1})$, $+0.302\,05 \times (d_{5/2},p_{3/2}^{-1})$, and $-0.186\,38(2s_{1/2},p_{3/2}^{-1})$. A normalization factor of 0.08 was required for the predicted 2^- cross

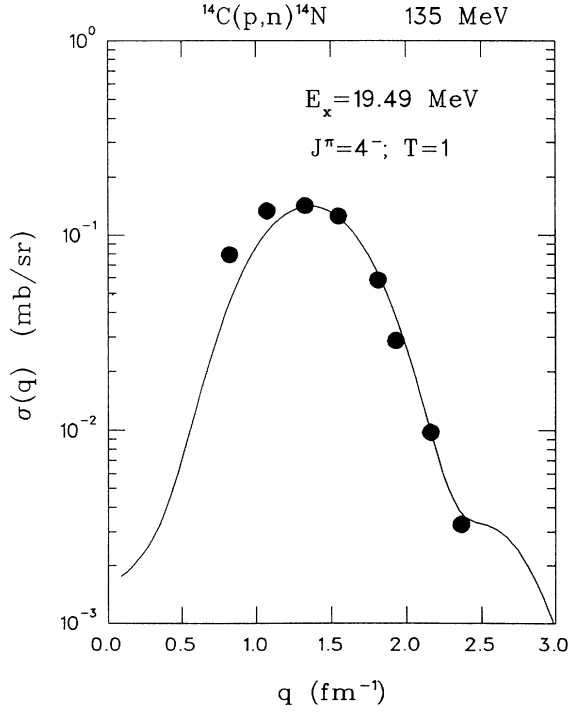

FIG. 6. Differential cross section measured for the 19.49 state in ^{14}N. The curve shows the DWIA calculation for the $1p_{3/2} \rightarrow 1d_{5/2}$ stretched transition from the ground state to the 4^- state, with b = 1.58 fm. The isovector transition strength to this state is $Z_1^2(\text{expt}) = 0.07$.

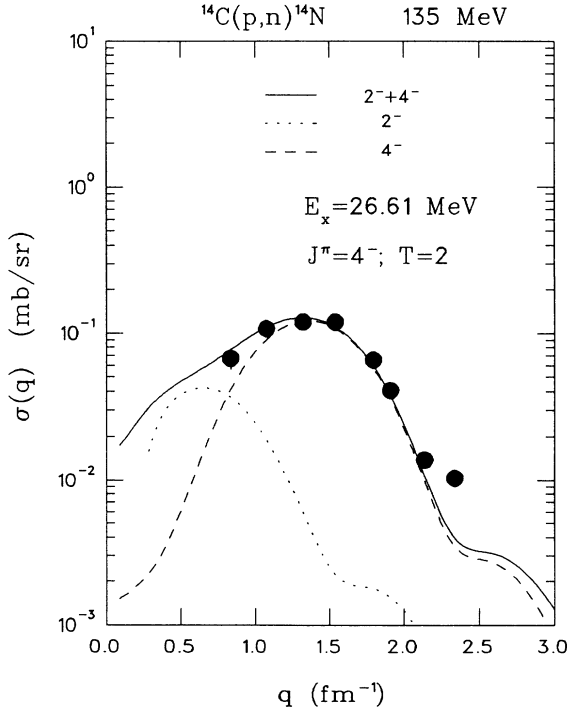

FIG. 7. Differential cross section measured for the 26.61 MeV state in ^{14}N. The curve shows the DWIA calculation for the $1p_{3/2} \rightarrow 1d_{5/2}$ stretched transition from the ground state to the 4^- state, with b = 1.58 fm. The isovector transition strength to this state is $Z_1^2(\text{expt}) = 0.06$.

section such that the $4^- + 2^-$ theoretical cross sections best describe the experimental result. The cross section for the 4^- state was normalized at $q = 1.9$ fm^{-1} data point where the contribution from the 2^- state is weak.

A. Extraction of the isovector strengths for the $0^+ \rightarrow 4^-$ transitions

From the normalization of the DWIA calculations to the experimental cross sections, assuming a $1p_{3/2} \rightarrow 1d_{5/2}$ single-particle transition, we obtain Z_1^2(expt), which is the square of the spectroscopic amplitude in the isospin representation [see Eq. (1)] for a transition from the 0^+ ground state of the target nucleus to a 4^- excited state of the residual nucleus. The DWIA calculations are normalized to the experimental cross sections near $q = 1.6$ fm^{-1}, where one expects the cross section to be mainly due to the stretched transition, as shown in Figs. 4–7. The isovector strengths that we determined for the 4^-;1 state at 13.76 MeV and for the 4^-;2 state at 26.61 MeV are upper bounds; the presence of unresolved states makes the determination of the isovector strengths more uncertain. Table II shows the isovector strength, Z_1^2(expt), obtained from this work. If we identify the isovector strength leading to the state at 15.88 MeV as being from the $1p_{3/2} \rightarrow 1d_{5/2}$ transition, its Z_1^2(expt) value is 0.03. Uncertainties associated with the experimental Z_1^2(expt) values are in the range of (10–20)%. The experimental Z_1^2 value is scaled by a factor of $(13/14)^3$ since the Z_1 appropriate for the relative coordinate (see the Appendix) is larger than the standard shell-model Z_1 by a factor of $(14/13)^{3/2}$.

B. Isospin assignments

The (p,n) reaction on a $T = 1$ target can excite $T = 0$, 1, and 2 states in the residual nucleus. The (e,e') reaction can excite only $T = 1$ and 2 states in ^{14}C, and, at backward angles, it is sensitive mainly to isovector transitions (by a factor of about 30 over the isoscalar transitions). The isobaric analog state (IAS) of the ground state of ^{14}C is known to be at 2.31 MeV in ^{14}N, and so excitation energies in the two nuclei are expected to be shifted by about this amount. From a comparison of the 4^- states obtained with the (p,n) and (e,e') reactions, the $T = 0$ states can be identified easily. For example, the analog of the 8.49 MeV state in ^{14}N is not observed in ^{14}C(e,e'); thus, the state at 8.49 MeV must have $T = 0$, as is well known. From a ^{14}B mass excess of 23.66 MeV [21], a ^{14}C mass excess of 3.13 MeV [21], a Coulomb energy difference of 2.99 MeV [assuming $E_C = 0.60z(z-1)/A^{1/3}$], the neutron-proton mass difference of 0.78 MeV, and the energy of the $T = 1$ ground-state analog in ^{14}N, we estimate that the analog of the $T = 2$ ^{14}B ground-state analog is located in ^{14}N at $E_x = 25.1$ MeV; thus, states in ^{14}N with an excitation energy less than about 25 MeV must have $T = 0$ or 1.

A direct method for the identification of the 4^-;1 and 4^-;2 states is based on a comparison of the (p,n) and (e,e') isovector strength, Z_1^2(expt). First, we need to establish the relationship between the amplitudes for the two probes. For a given stretched transition with spin transfer ΔJ and isospin transfer ΔT, the nuclear transition density is the same for the different probes, except for an isospin coefficient in the spectroscopic amplitude, $Z_{\Delta T}$, given by

$$Z_{\Delta T} = \sqrt{\frac{2\Delta T + 1}{(2J_i + 1)(2T_f + 1)}} \langle T_i T_{3i} \Delta T \Delta T_3 | T_f T_{3f} \rangle \times A(\Delta J, \Delta T) \ , \quad (1)$$

where

$$A(\Delta J, \Delta T) = \frac{\langle J_f T_f || [a^\dagger_{j_p} \times \tilde{a}_{j_h}]^{\Delta J, \Delta T} || J_i T_i \rangle}{\sqrt{2\Delta T + 1}\sqrt{2\Delta J + 1}} \quad (2)$$

is the OBDME, reduced in both isospin and angular momentum in the convention of Edmonds [29]. Using the values $T_i = 1$ and $T_{3i} = 1$ for the target, $\Delta T = 1$ for the (p,n) and the (e,e') reactions, with $\Delta T_3 = -1$ and $\Delta T_3 = 0$, respectively, and the desired T_f, in these equations, we obtain

$$Z_1^{(p,n)} = Z_1^{(e,e')} \text{ for } T = 1 \ , \quad (3)$$

$$Z_1^{(p,n)} = \frac{Z_1^{(e,e')}}{\sqrt{3}} \text{ for } T = 2 \ . \quad (4)$$

TABLE II. Experimental isovector strengths for the transitions from the ground state of ^{14}C to the 4^- states in ^{14}N with the (p,n) reaction, and analog 4^- states in ^{14}C, with (e,e') scattering. The states in ^{14}N lie at excitation energies ~2.3 MeV above the excitation energy of the analog candidate in ^{14}C.

		^{14}C$(p,n)^{14}$N				^{14}C(e,e') [a]	
E_x(MeV)	T	Z_1^2(expt)	Z_1^2(expt)/$\sum(Z_{1T}^2)_{\rm ESPM}$	E_x(MeV)	T	Z_1^2(expt)	Z_1^2(expt)/$\sum(Z_{1T}^2)_{\rm ESPM}$
8.49	0	0.22	0.66				
			$\sum(T=0) = 0.66$				
13.76	1	0.10	0.20	11.7	1	0.10	0.20
19.49	1	0.07	0.14	17.3	1	0.08	0.16
			$\sum(T=1) = 0.34$				$\sum(T=1) = 0.36$
26.61	2	0.06	0.36	24.4	2	0.20	0.40
			$\sum(T=2) = 0.36$				$\sum(T=2) = 0.40$

[a] Ref. [5].

By comparing the third and seventh columns of Table II, which show the isovector strength, $Z^2_{\Delta T}$(expt), seen with the (p,n) reaction and that seen with (e,e') scattering, and squaring both sides of Eq. (3), we can assign the 4^- states at 13.76 MeV and 19.49 MeV to have $T = 1$. In a similar fashion, the 4^- state at 26.61 MeV can be assigned to have $T = 2$ [using Eq. (4)]. Confirmation of the $T = 2$ assignment is anticipated to come from a $^{14}C(n,p)^{14}B$ experiment [22].

V. OTHER STATES SEEN AT LARGE MOMENTUM TRANSFER

At momentum transfers between 1.3 and 2.5 fm^{-1}, where the cross sections for the 4^- states are largest, we extracted differential cross sections for all observed excitations. The spin and isospin of the energy levels up to 10 MeV in ^{14}N are well known and we can identify our observed levels in this excitation energy region with known states listed in the latest compilation of ^{14}N states [12]. These states are as follows: 0.00 MeV (1^+;0), 2.31 MeV (0^+;1), 3.95 MeV (1^+;0), 5.10 MeV (2^-;0), 5.78 MeV (3^-;0), and 7.00 MeV (2^+;0). The angular distributions for these states are presented in Ref. [23]. Above 10 MeV of excitation energy in ^{14}N we see peaks at 10.43, 11.67, 12.69, and 15.88 MeV.

The measured differential cross section and the DWIA calculation for the state at 10.43 MeV are shown in Fig. 8. The compilation of Ajzenberg-Selove [12] lists a 2^+;1 state at 10.432 MeV. Our shell-model calculation predicts the first 2^+;1 at 9.30 MeV. The OBDME's for the transition to this state were employed in the DWIA calculation producing the cross section shown in Fig. 8 (dotted curve). An overall normalization factor of 0.18 was required. From the $^{14}C(e,e')$ results [5] the analog of this state is at 8.318 MeV. The form factor for the 2^+ in the $^{14}C(e,e')$ work employed OBDME's obtained from a $2\hbar\omega$ shell-model calculation. We employed these matrix elements in the DWIA calculation and obtained the cross section shown by the dashed curve in Fig. 8. This calculation describes the experimental results reasonably well at large momentum transfer and does not require a normalization factor, showing for this case the importance of including the $2\hbar\omega$ amplitudes in the calculations.

Figure 9 shows the experimental cross section for the peak at 11.67 MeV. This energy is consistent with that for a known 1^- or 2^- state at 11.676 MeV [12]. Our shell-model calculations predict a 1^-;1 state at 12.53 MeV, a 2^-;0 state at 11.71 MeV, and a 2^-;1 state at 11.99 MeV. Although the energies of these model states are consistent with that of the observed peak, the OBDME's obtained from this calculation do not describe the experimental cross sections well.

Figure 10 shows the experimental and theoretical cross sections for the 12.69 MeV state which is described as a 3^-;0 state. The compilation of ^{14}N energy levels [12] lists a 3^-;0 at 12.690 MeV. A 4^-;0 assignment was given to an excitation seen at 12.79 MeV in the $^{14}N(\pi,\pi')$ reaction [24]; however, it is unlikely that this is the analog of the state that we see given the energy difference. The shell-

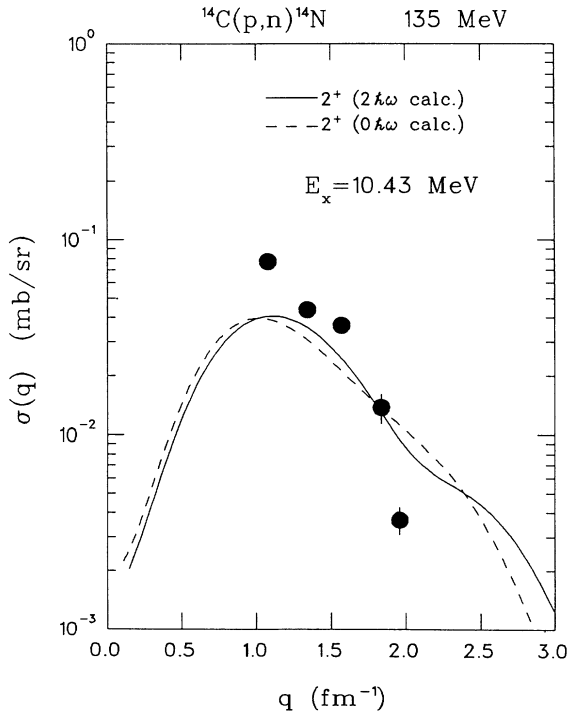

FIG. 8. Differential cross section measured for the 10.43 MeV state in ^{14}N. The curve shows a DWIA calculation for the transition to the 2^+;1 state employing OBDME's obtained from a shell-model calculation.

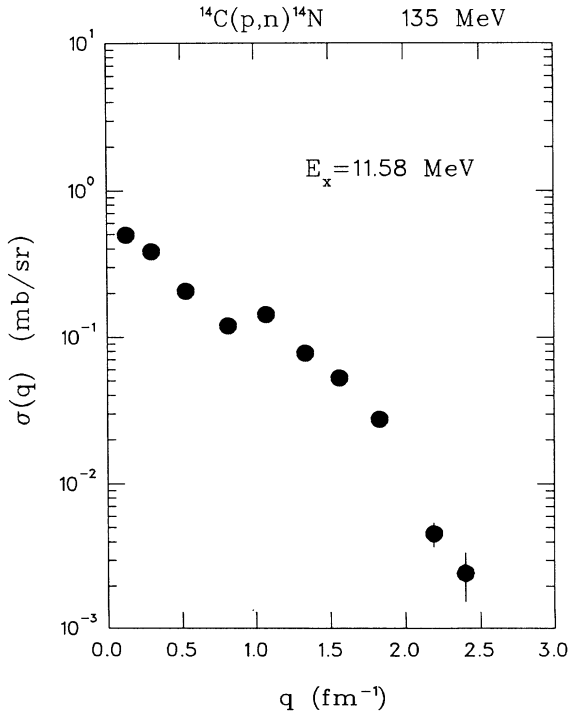

FIG. 9. Differential cross section measured for the 11.67 MeV excitation. This energy is consistent with a 1^- state and a 2^- state (see text).

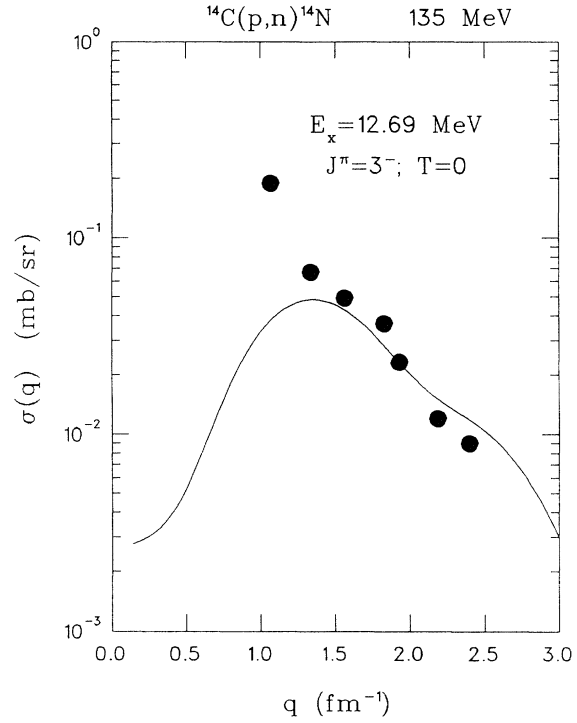

FIG. 10. Differential cross section measured for the 12.69 MeV state in ^{14}N. The curve shows a DWIA calculation for the $1p_{3/2} \rightarrow 1d_{5/2}$ transition to the $3^-;0$ state.

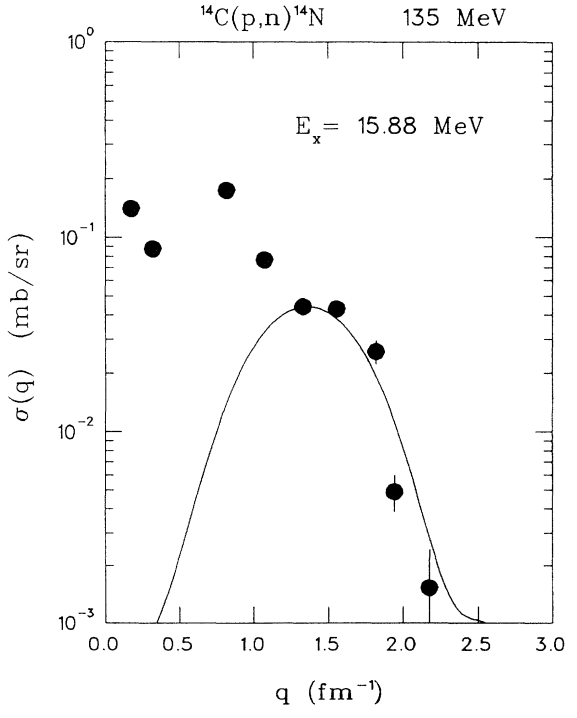

FIG. 11. Differential cross section measured for the 15.88 MeV state in ^{14}N. The curve shows the DWIA calculation for the $1p_{3/2} \rightarrow 1d_{5/2}$ stretched transition from the ground state to the 4^- state, with $b = 1.58$ fm. The isovector transition strength to this state is $Z_1^2(\text{expt}) = 0.03$.

model calculation described in Sec. VI predicts a $3^-;0$ state at 13.25 MeV. The OBDME's for the transition to this state produce a cross section that does not describe the experimental result. From a weak-coupling calculation for $A = 14$ nuclei [25], a $3^-;0$ model state with a predominant $(d_{5/2})(p_{1/2}^{-1})$ configuration was identified as the state at 12.690 MeV. A $1p_{1/2} \rightarrow 1d_{5/2}$ transition in the DWIA calculation produces a cross section that has the appropriate shape but requires a normalization of 0.10.

The peak at 15.88 MeV seems also to be a complex, and we are unable to describe it completely. The large momentum transfer region is described reasonably well by a $1p_{3/2} \rightarrow 1d_{5/2}$ 4^- DWIA calculation; we tentatively identify this excitation as a 4^- state (see Fig. 11).

VI. SHELL-MODEL CALCULATIONS

In the extreme single-particle model (ESPM), the configuration of the 0^+ ground state of ^{14}C is $\pi p_{1/2}^{-2}$ and that for the 4^- excited states is $(\pi d_{5/2})(\nu p_{3/2}^{-1})(\pi p_{1/2}^{-2})$. With this description, we obtain the following sum rules for the isovector strength for the transitions to the 4^- states:

$$\sum (Z_{1T}^2)_{\text{ESPM}} = \frac{3n_h - p_h}{6(2j_h+1)} = \frac{1}{3} \text{ for } T = 0 , \quad (5)$$

$$\sum (Z_{1T}^2)_{\text{ESPM}} = \frac{n_h}{2(2j_h+1)} = \frac{1}{2} \text{ for } T = 1 , \quad (6)$$

$$\sum (Z_{1T}^2)_{\text{ESPM}} = \frac{p_h}{6(2j_h+1)} = \frac{1}{6} \text{ for } T = 2 , \quad (7)$$

where j_h is the total angular momentum of the $1p_{3/2}$ hole orbital, and n_h and p_h are respectively the number of neutrons and protons in that orbital. Table II lists E_x, $Z_1^2(\text{expt})$, T, and $Z_1^2(\text{expt})/\sum(Z_{1T}^2)_{\text{ESPM}}$, for the $T = 0$, 1, and 2 4^- candidates observed with the (p,n) and (e,e') reactions. The reduction of total isovector strength with respect to the ESPM result is larger for the $T = 1$ and $T = 2$ components than for the $T = 0$ component. The total isovector strength for the $T = 1$ component obtained with the (p,n) reaction with respect to the ESPM is 0.34, which is in good agreement with the value 0.36 obtained in the ^{14}C(e,e') analysis [5] (assuming no contribution from meson-exchange currents). For the $T = 2$ component, we observe $Z_1^2(\text{expt})/\sum(Z_{1T}^2)_{\text{ESPM}} = 0.36$ while the (e,e') analysis finds 0.40, also in reasonably good agreement.

Shell-model calculations that include residual interactions and ground-state correlations were performed with the code OXBASH [17]. The even-parity states (including the ground state) were formed by confining the active nucleons to the p shell ($0\hbar\omega$ model space) while the odd-parity states were formed by allowing one nucleon to be excited to the sd shell ($1\hbar\omega$ model space). The Cohen-Kurath interaction [CK(pot)] [26] was used for the p shell matrix elements and the Millener-Kurath interaction [27] was used for the p- to sd-shell matrix elements. This ba-

TABLE III. Experimental Z_1^2(expt) and predicted Z_1^2(calc) (from large-basis shell-model calculations) isovector strengths for the transitions from the 0^+ ground state of ^{14}C to the 4^- states in ^{14}N.

Experimental			Predicted		
E_x(MeV)	T	Z_1^2(expt)	E_x(MeV)	T	Z_1^2(calc)
8.49	0	0.22	8.51	0	0.20
			11.38	0	0.03
			14.20	0	0.02
			23.49	0	0.04
		$\sum Z_1^2$(expt)=0.22			$\sum Z_1^2$(calc)=0.29
13.76	1	0.10	13.54	1	0.23
			15.03	1	0.03
19.49	1	0.07	17.74	1	0.15
			18.79	1	0.01
		$\sum Z_1^2$(expt)=0.17			$\sum Z_1^2$(calc)=0.42
26.61	2	0.06	25.68	2	0.14
		$\sum Z_1^2$(expt)=0.06			$\sum Z_1^2$(calc)=0.14

sis is the same as that adopted by Plum *et al.* [5] and Holtkamp *et al.* [6] to describe inelastic electron and pion scattering of the analog 4^- states in ^{14}C. For the ground state, the calculated occupation of the $p_{3/2}$ orbital is 7.67 nucleons and that of the $p_{1/2}$ orbital is 2.33 nucleons.

The identification of a particular model state with a given experimental 4^- candidate was based on a comparison of excitation energies, provided that the theory describes the corresponding differential cross section reasonably well. The shell-model calculation for the $4^-;0$ states predicts ten levels in the excitation-energy region from 8 to 24 MeV. Based on the experimentally deter-

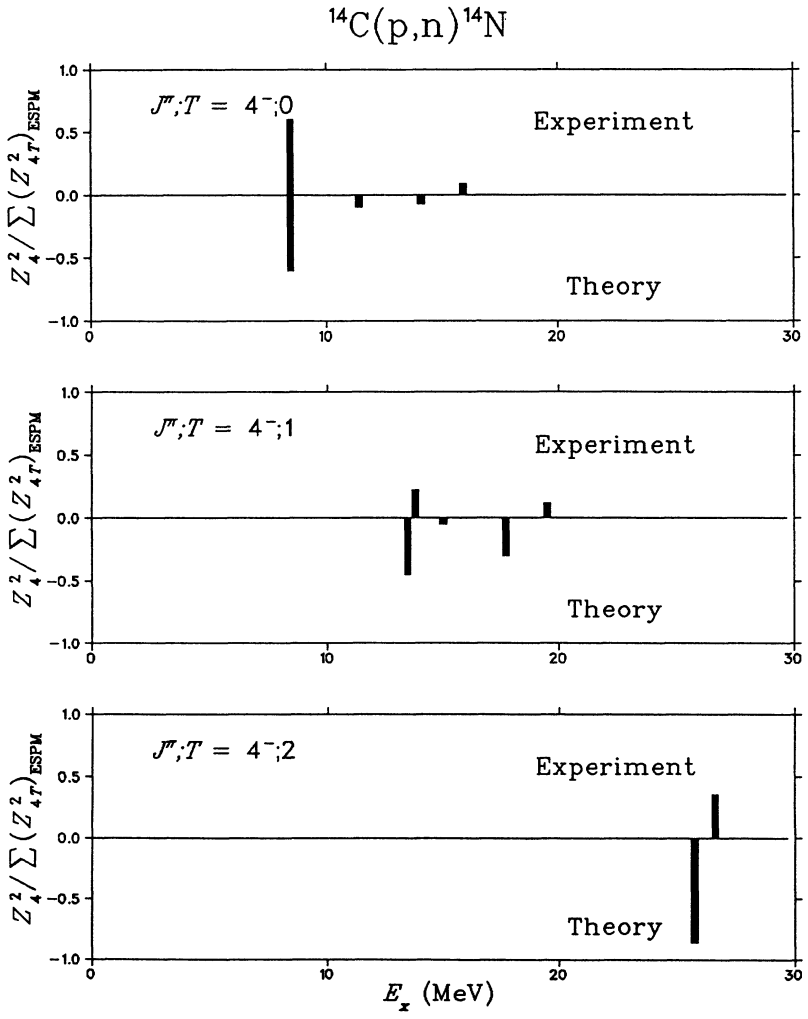

FIG. 12. Fraction of the ESPM isovector strengths, $Z_1^2(\text{expt})/\sum(Z_{1T}^2)_{\text{ESPM}}$, obtained with the (p,n) reaction, compared with shell-model predictions, $Z_1^2(\text{calc})/\sum(Z_{1T}^2)_{\text{ESPM}}$, for the transitions from the 0^+ ground state of ^{14}C to the 4^- $T = 0$, 1, and 2 components in ^{14}N.

mined excitation energy and transition strength to the 8.49 MeV level, we identify the model state at 8.51 MeV with this state. All of the other transition strengths leading to $4^-;0$ states predicted by the shell-model calculation are too weak to be measured. The total isovector transition strength to all the $4^-;0$ model states is 0.29; thus for the transitions to the $4^-;0$ states we see 66% of the ESPM value and 76% of the shell-model value. Calculated excitation energies and Z_1^2(calc) are listed in Table III and the calculated and observed isovector strengths for the $4^-;0$ states are compared in Fig. 12.

The shell-model calculation for the $4^-;1$ states predicts ten levels in the excitation energy region from 13 to 25 MeV. We identify the first $4^-;1$ model state at 13.54 MeV with our first $4^-;1$ state at 13.76 MeV. The shell-model calculation predicts a $4^-;1$ level at 19.82 MeV that could correspond to our $4^-;1$ state at 19.58 MeV; however, the predicted strength for this transition is very small. Only the transition amplitude to the 4^- state predicted at 17.74 MeV can produce a measurable cross section. The total predicted isovector transition strength to all the $4^-;1$ model states is 0.42; hence, for these transitions we see 34% of the ESPM and 41% of the shell-model result (see Fig. 12).

The shell-model calculation for the $4^-;2$ states predicts five levels in the excitation energy region from 25 to 40 MeV. From this calculation, only the model state at 25.68 MeV has the strength to be identified with our $4^-;2$ state at 26.61 MeV. The total isovector strength for this model state is 0.14; therefore, for the transitions to the $4^-;2$ states we see 36% of the ESPM and 43% of the shell-model result (see Fig. 12).

This $0\hbar\omega+1\hbar\omega$ shell-model calculation predicts many 4^- states. As mentioned previously, the $0\hbar\omega$ model space seems to be too limited for the even-parity states. Including $2\hbar\omega$ components in the ground-state wave function will result in even more fragmentation for the 4^- states. The mixing of the $1p3h$ $1\hbar\omega$ configurations with the $3p5h$ $3\hbar\omega$ configurations will result in more fragmentation for the 4^- states and in a redistribution of the isovector strength. Many of these states will be too weak to be observed experimentally, and the larger model space will have the net effect of lowering the value of the total predicted isovector strength. Such calculations are beyond the scope of this work.

VII. CONCLUSIONS

Experimentally we observed one $4^-;0$ state at 8.49 MeV with an isovector strength, Z_1^2(expt) = 0.22; we observed two $4^-;1$ states at 13.76 and 19.49 MeV with isovector strengths, Z_1^2(expt) = 0.10 and 0.07, respectively; and we observed one $4^-;2$ state at 26.61 MeV with an isovector strength, Z_1^2(expt) = 0.06. These isovector strengths for the transitions to the $4^-;1$ and $4^-;2$ states agree very well with the isovector strengths for the transitions to their analog states determined in a $^{14}C(e,e')$ analysis. These results assume that the lower-multipolarity states in the complexes are described well by our shell-model calculations.

If the ground state of ^{14}C is described within the p shell, then the amplitude for the $1p_{3/2} \rightarrow 1d_{5/2}$ stretched transition is expected to be the only important contribution to excite the 4^- states. Our results provide a good test for shell-model calculations. The experimental results show that the $0\hbar\omega+1\hbar\omega$ shell-model calculations predict the correct isovector strength for the transition to the $4^-;0$ state; however, these calculations overpredict the isovector strength for the transitions to each of the $4^-;1$ and $4^-;2$ states by at least a factor of 2. These results suggest that the $4^-;0$ state at 8.49 MeV has primarily a $1p3h$ configuration, whereas the $4^-;1$ states at 13.76 MeV and 19.49 MeV, and the $4^-;2$ state at 26.61 MeV probably include significant $3p5h$ configurations. The mixing of $1p3h$ and $3p5h$ configurations will result in more fragmentation for the 4^- states; therefore, these calculations must include the *sd*-shell for the ground-state wave function.

Other odd-parity states such as the 1^-, 2^- states at 11.67 MeV and the $3^-;0$ state at 12.69 MeV have more complex configurations, and were experimentally unresolved from other states in this reaction, making more difficult the interpretation of the shell-model results.

The even-parity states such as the $1^+;1$ state at 13.74 MeV and the $2^+;1$ state at 10.43 MeV have angular distributions that are described reasonably well by the shell-model calculations; however, the $0\hbar\omega$ shell-model results require large normalization factors. If the OBDME's from the $2\hbar\omega$ shell-model calculation described in the $^{14}C(e,e')$ analysis are used in the DWIA calculations, then there is better agreement with experiment.

ACKNOWLEDGMENT

This work was supported in part by the National Science Foundation.

APPENDIX

In this appendix we discuss the center-of-mass corrections that must be applied to shell-model one-body density-matrix elements from OXBASH, in the form of the Z coefficients of Eq. (1), for input to the distorted-wave code DW81 [14]. A more detailed discussion is given in an appendix to Ref. [20].

When harmonic-oscillator wave functions are employed, center-of-mass corrections to electron scattering form factors are easily made by including the Tassie-Barker correction [28]. Implicit in this correction is the use of conventional shell-model OBDME and radial transition densities in which the coordinates of nucleons are referred to an arbitrary origin and the harmonic-oscillator parameter is given by $b_o^2 = \hbar/m\omega$, where m is the nucleon mass.

The situation for the distorted-wave code DW81 is somewhat different since the internal integrations are over the distorted-wave coordinate and the coordinate of a nucleon relative to the $A-1$ core. This calls for the radial transition density to be expressed in terms of

the relative coordinate. Again, for harmonic-oscillator wave functions, this transformation from the pair of coordinates (r_i, R_{A-1}) to (r_{iC}, R_A), where $C = A - 1$, can be made. For stretched transitions involving orbits with Q_1 and Q_2 oscillator quanta, this transformation simply introduces a multiplicative factor $[A/(A-1)]^{(Q_1+Q_2)/2}$ into the OBDME or the transition density. The transition density is expressed in terms of harmonic-oscillator wave functions with arguments $r_{iC}/b_{\rm rel}$, where $b_{\rm rel}$ is the relative oscillator parameter $b_{\rm rel} = \sqrt{A/(A-1)}b_o$ ($b^2_{\rm rel} = \hbar/\mu\omega$ with μ the nucleon reduced mass). The multiplicative factor should be applied to the conventional Z coefficients of Eq. (1) for input to DW81. Conversely, the factor should be removed from a Z coefficient extracted by normalizing DW81 cross sections to data if one wants the conventional shell-model Z coefficient.

[1] R. A. Lindgren, W. J. Gerace, A. D. Bacher, W. G. Love, and F. Petrovich, Phys. Rev. Lett. **42**, 1524 (1979).

[2] J. J. Kelly, Ph.D. thesis, Massachusetts Institute of Technology, 1981.

[3] B. D. Anderson, J. W. Watson, and R. Madey, in *Nuclear Structure at High Spin, Excitation, and Momentum (McCormick's Creek Park, Bloomington, Indiana)*, Proceedings of the Workshop on Nuclear Structure at High Spin, Excitation, and Momentum Transfer, edited by H. Nann, AIP Conf. Proc. No. 142 (AIP, New York, 1985), p. 155.

[4] R. A. Lindgren, J. Phys. (Paris) Colloq. **45**, C4-443 (1984).

[5] M. A. Plum, R. A. Lindgren, J. Dubach, R. S. Hicks, R. L. Huffman, B. Parker, G. A. Peterson, J. Alster, J. Lichtenstadt, M. A. Moinester, and H. Baer, Phys. Rev. C **40**, 1861 (1989).

[6] D. B. Holtkamp, S. J. Seestrom-Morris, D. Dehnhard, H. W. Baer, C. L. Morris, S. J. Greene, C. J. Harvey, D. Kurath, and J. A. Carr, Phys. Rev. C **31**, 957 (1985).

[7] C. Lebo, B. D. Anderson, T. Chittrakarn, A. R. Baldwin, R. Madey, J. W. Watson, and C. C. Foster, Phys. Rev. C **38**, 1099 (1988).

[8] B. D. Anderson, T. Chittrakarn, A. R. Baldwin, R. Madey, J. W. Watson, and C. C. Foster, Phys. Rev. C **31**, 1147 (1985).

[9] A. R. Baldwin and R. Madey, Nucl. Instrum. Methods **171**, 149 (1980).

[10] R. Madey, J. W. Watson, M. Ahmad, B. D. Anderson, A. R. Baldwin, A. L. Casson, R. A. Cecil, A. Fazeley, J. M. Knudson, C. Lebo, W. Pairsuwan, P. J. Pella, J. C. Varga, and T. R. Witten, Nucl. Instrum. Methods **214**, 401 (1983).

[11] J. J. Kelly, computer code ALLFIT (unpublished).

[12] F. Ajzenberg-Selove, Nucl. Phys. **A523**, 76 (1991).

[13] P. J. Brussaard and P. W. M. Glaudemans, *Shell-Model Applications in Nuclear Spectroscopy* (North-Holland, Amsterdam, 1977).

[14] J. R. Comfort (unpublished).

[15] M. A. Franey and W. G. Love, Phys. Rev. C **31**, 488 (1985).

[16] J. R. Comfort and B. C. Karp, Phys. Rev. C **21**, 2162 (1980).

[17] B. A. Brown, A. Etchegoyen, W. D. M. Rae, and N. S. Godwin, computer code OXBASH (unpublished).

[18] R. W. Detenbeck, J. C. Armstrong, A. S. Figuera, and J. B. Marion, Nucl. Phys. **72**, 552 (1965).

[19] D. J. Millener, J. W. Olness, and E. K. Warburton, Phys. Rev. C **28**, 497 (1983).

[20] F. P. Brady, T. D. Ford, G. A. Needham, J. L. Romero, D. S. Sorenson, C. M. Castaneda, J. L. Drummond, E. L. Hjort, B. McEachern, N. S. P. King, and D. J. Millener, Phys. Rev. C **43**, 2284 (1991).

[21] A. H. Wapstra and K. Bos, At. Data Nucl. Data Tables **19**, 175 (1977).

[22] X.-D. Hu (private communication).

[23] L. A. C. Garcia, Ph.D. thesis, Kent State University, 1992.

[24] D. F. Geesaman, D. Kurath, G. C. Morrison, C. Olmer, B. Zeidman, R. E. Anderson, R. L. Boudrie, H. A. Thiessen, G. S. Blanpied, G. R. Burleson, R. Segel, and L. W. Swenson, Phys. Rev. C **27**, 1134 (1983).

[25] S. Lie, Nucl. Phys. **A181**, 517 (1972).

[26] S. Cohen and D. Kurath, Nucl. Phys. **A73**, 1 (1965).

[27] D. J. Millener and D. Kurath, Nucl. Phys. **A255**, 315 (1975).

[28] L. T. Tassie and F. C. Barker, Phys. Rev. **111**, 940 (1958).

[29] A. R. Edmonds, *Angular Momentum in Quantum Mechanics* (Princeton University Press, Princeton, NJ, 1957).